Liquid-crystal-based biosensing beyond texture observations

Mon-Juan Lee[a,*], Chi-Hao Lin[b], and Wei Lee[b,**]
[a]Department of Bioscience Technology, Chang Jung Christian University, Guiren Dist., Tainan 71101, Taiwan
[b]College of Photonics, National Chiao Tung University, Guiren Dist., Tainan 71150, Taiwan

ABSTRACT

The texture observation has long been the core technique in liquid crystal (LC)-based biosensing. One of the drawbacks of this observational means is the difficulty in quantitative analysis. In this invited paper, we report on our recent attempt to improve the LC-based biosensing technique through the analysis of bovine serum albumin (BSA), a protein standard commonly used in the assay of protein concentration. We propose to overcome the technical limitations in the analysis of LC-based biosensors by considering alternative measuring schemes. By means of the induced changes in electro-optical properties of LCs in the presence of different concentrations of BSA, novel quantitative techniques specific for LC-based biosensors are developed.

Keywords: Liquid crystals, Electro-optical properties, Biophotonics, Biosensors, Bovine serum albumin, Protein

1. INTRODUCTION

The sensitivity and effectiveness of liquid crystal (LC)-based biosensors have been demonstrated by the increasing number of studies in recent years. The birefringent properties of the anisotropic mesogenic molecules are exploited to detect biomolecules, as well as their binding and reaction with other molecules, which disturb the director orientation and trigger change in optical appearance of LCs. Currently, LC-based biosensing techniques are developed for the signal amplification of protein–peptide, protein–protein and protein–receptor binding,[1–4] real-time monitoring of enzymatic reactions,[5,6] recognition of the orientation of immobilized proteins,[7,8] immunodetection of the specific binding between antigens and antibodies,[9–16] glucose biosensing,[17] and DNA hybridization assays.[18–20]

Results from our previous reports suggest that, by applying HDN, a nematic LC with wide nematic range and large birefringence (Δn = 0.333), and by ultraviolet modification of the monolayer of *N*,*N*-dimethyl-*n*-octadecyl-3-aminopropyltrimethoxysilyl chloride (DMOAP), which serves as the alignment layer for LCs, the detection limit for the cancer biomarker CA125 was drastically improved in comparison with label-based fluorescence immunoassay and the common LC-based immunodetection with 4-cyano-4'-pentylbiphenyl (5CB) as the sensing element.[15,16] As the change in optical textures of LCs can only provide qualitative description of the immunoreaction, we determined the relative intensity of the optical texture of LCs by an image processing software to correlate the results of LC-based immunoassay quantitatively with the concentration of CA125.[14] However, due to the uneven distribution of biomolecules on the alignment layer, variations in the quantitative results between individual experiments rendered this method impractical.

In this study, we propose to overcome the technical limitations in the quantitative analysis of LC-based biosensing by taking advantage of the electro-optical and electric capacitance properties of LCs, which are expected to change in the presence of different concentrations of biomolecules. Bovine serum albumin (BSA), a protein standard commonly used in the quantification of protein concentration, was spin-coated on DMOAP-coated glass substrates embedded with indium–tin-oxide (ITO) electrodes to produce a uniformly distributed layer of protein in an attempt to reduce variation in quantitative results (Fig. 1). The change in electro-optical properties of LCs with increasing voltage was monitored when an external alternating current (ac) field was applied. It is expected that, by investigating the correlation of BSA concentrations with the electro-optical and electric capacitance parameters of LCs, novel quantitative techniques specific for LC-based biosensing can be developed.

*mjlee@mail.cjcu.edu.tw; phone +886 (0)6 278-5123 ext. 3212; fax +886 (0)6 278-5010
**wlee@nctu.edu.tw; phone +886 (0)6 303-2121 ext. 57826; fax +886 (0)6 303-2535

Liquid Crystals XIX, edited by Iam Choon Khoo, Proc. of SPIE Vol. 9565, 956510
 · doi: 10.1117/12.2187818

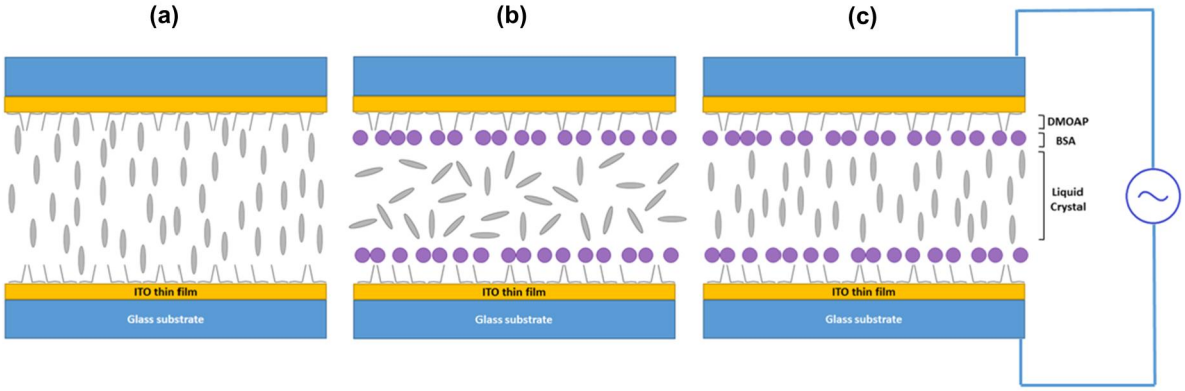

Figure 1. Schematic of LC-based biosensing and its quantitation by measuring the electro-optical and electric capacitance properties of LCs. (a) LC molecules are aligned perpendicularly to the glass surfaces covered by the DMOAP alignment layers in the absence of BSA. (b) In the presence of BSA (represented by balls), the alignment of LCs is disrupted. (c) When an external ac field is applied, reorientation of LC molecules is induced and the original alignment can be restored at high voltages. As the concentration of BSA increases, a higher voltage is required to restore the vertical alignment of LC molecules. The change in the electro-optical and electric capacitance properties of LCs as a function of voltage can thus be exploited to determine the concentration of BSA.

2. METHODOLOGY

2.1 Materials

Glass slides coated with indium–tin-oxide (ITO) electrodes were obtained from Mesostate International Co., Ltd. The silane surfactant dimethyloctadecyl[3-(trimethoxysilyl)propyl]ammonium chloride (DMOAP) and bovine serum albumin (BSA, 66 kDa) lyophilized powder were both purchased from Sigma–Aldrich. HDN, a eutectic nematic mixture of LCs (Δn = 0.333 at the wavelength of 589.3 nm and the temperature of 20 °C), was provided by Jiangsu Hecheng Display Technology Co., Ltd. The dielectric constants along and perpendicular to the nematic director are 14.8 and 4.4 at 1 kHz and 20 °C, respectively.

2.2 Preparation of DMOAP-coated glass slides

The glass slides were cleaned by immersing successively in aqueous solutions of detergent, deionized (DI) water and 99% ethanol, with each step accompanied by ultrasonication for 15 min at room temperature. The glass slides were dried under a stream of nitrogen and then baked at 74 °C for 15 min. The cleaned glass slides were immersed in an aqueous solution of 1% (v/v) DMOAP for 15 min at room temperature, rinsed with DI water for 1 min to remove excess DMOAP, followed by drying under a stream of nitrogen and heating at 100 °C for 15 min.

2.3 Immobilization of BSA by spin-coating

The BSA solutions of desired concentrations were prepared by dissolving the lyophilized powder of BSA in DI water, followed by sequential dilution. On a spin-coater (APISC), 200 μl of BSA solution was deposited on the center of a DMOAP-coated ITO glass slide, which was spun at 500 rpm for 20 sec at room temperature. The coating procedure was repeated 20 times so that a thin film of BSA was uniformly distributed on the DMOAP alignment layer.

2.4 Assembly of the LC cell

Each LC optical cell was assembled by pairing two ITO glass slides coated with DMOAP (and BSA). LC cell spacers of 5 μm in average size were prepared in ethanol and dispensed on the four corners of one of the glass slides, which was allowed to dry at room temperature for 5 min. The glass slide was then covered with the other BSA/DMOAP-coated glass slide, sealed with AB glue and dried at room temperature for another 2 h. Finally, the empty cell was filled with LC by capillary action. The optical texture of LCs was observed under a crossed polarized microscope in the transmission mode with an exposure time of 14.84 ms.

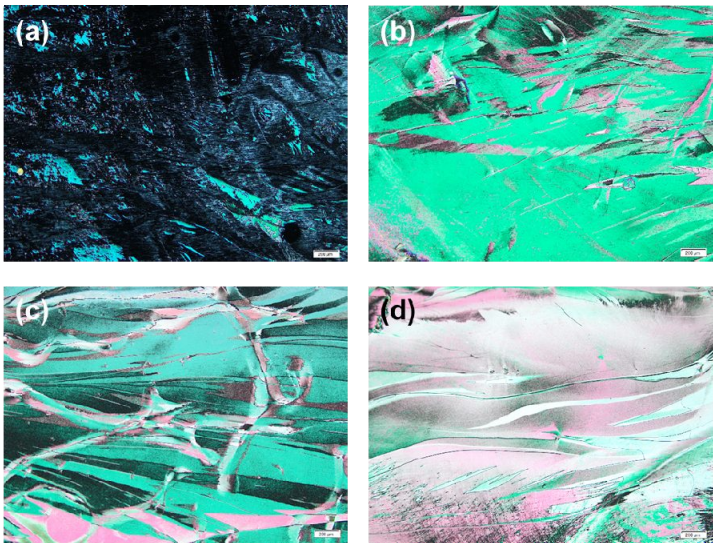

Figure 2. Optical textures of LCs in the presence of (a) 1, (b) 10, (c) 100-μg/ml and (d) 1-mg/ml BSA spin-coated on DMOAP-layered ITO glass substrates. Scale bar, 200 μm.

2.5 Electro-optical and electric capacitance measurements

Electro-optical (i.e., voltage-dependent transmittance) measurements were carried out by installing the LC cell between two crossed polarizers, with the projection of the LC director onto the substrate plane and the transmission axis of either polarizer intersected at 45°. A He–Ne laser operating at 633 nm was used as a probe for characterizing the optical transmission properties, and the transmitted light intensity was monitored by a photodiode detector. A Tektronix arbitrary function generator (AFG 320) was utilized to apply an ac voltage of 1–10 V at 1 kHz across the cell thickness, and a computer-controlled LabVIEW data acquisition system was used to collect and process the signal from the photodiode detector. In addition, a high-precision LCR meter (Agilent E4980A), which generates an ac voltage of 1–15 V at 1 kHz, was applied to measure the voltage-dependent electrical capacitance of the LC cell.

3. RESULTS AND DISCUSSION

3.1 Optical textures of LC in the presence of various concentrations of BSA

BSA solutions of 1, 10, 100 μg/ml and 1 mg/ml were spin-coated on DMOAP-coated ITO glass slides and detected with LC under a crossed polarized microscope. In the absence of BSA, the homeotropic alignment of the nematic LC resulted in an optical texture that was completely dark. With an increasing concentration of BSA adsorbed to DMOAP, the LC alignment was disrupted to a greater extent, and the optical texture changed from the dark state to a brighter appearance (Fig. 2). These results suggest that the optical response of the LC is sensitive to the amount of biomolecules present.

3.2 Voltage dependence of the optical transmittance of LC in the presence of various concentrations of BSA

In order to study the correlation between BSA concentration and the optical transmittance of HDN, the BSA-coated LC cells were subjected to an ac field, and the change in optical transmittance of each LC cell with increasing voltage from 0 to 10 V was monitored. As the BSA concentration increases, more LC molecules were disrupted by BSA to orient themselves in various directions and tilt angles. Consequently, the voltage and total available phase change to revert the LC molecules from a tilted state to the homeotropic alignment increased with increasing concentration of BSA (Fig. 3). The phase retardation δ deduced from the voltage-dependent transmittance (V–T) curve can be used to calculate the effective birefringence Δn_{eff} of LC with the following equation:

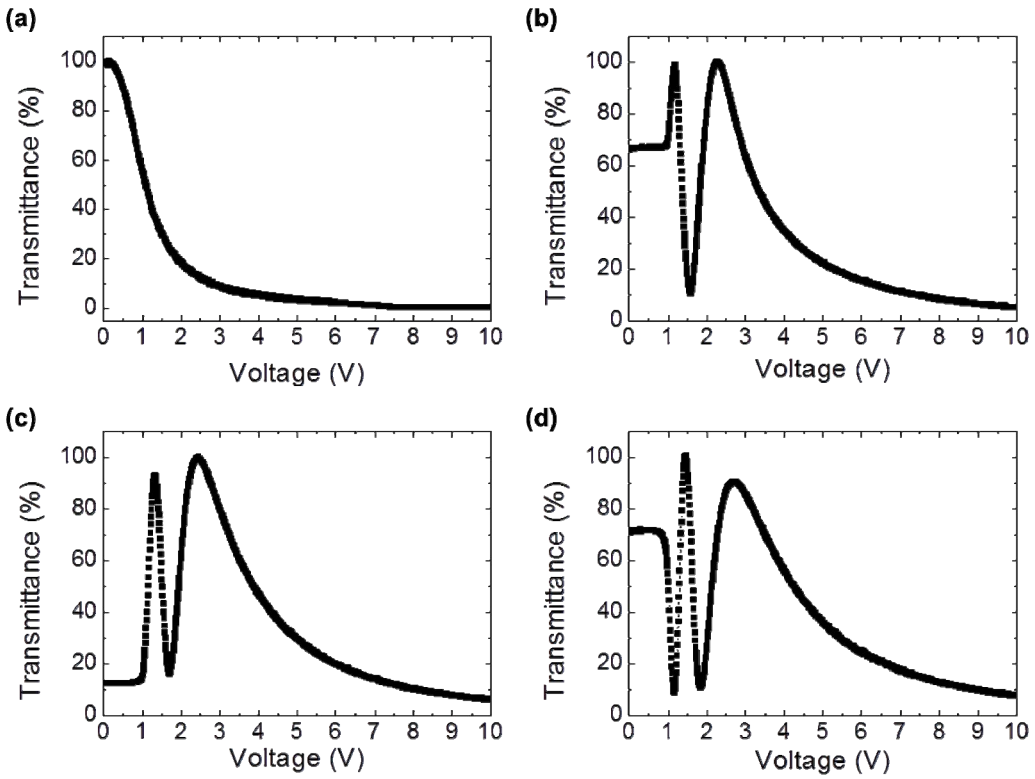

Figure 3. Voltage dependence of the optical transmittance of LCs in the presence of (a) 1, (b) 10, (c) 100 μg/ml and (d) 1 mg/ml of BSA spin-coated on DMOAP-covered ITO glass substrates. $d = 5.4 \pm 0.1$ μm.

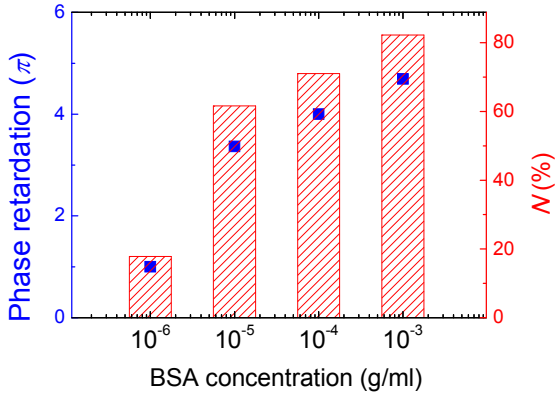

Figure 4. Correlation of the electro-optical parameters of LCs acquired from *V–T* measurement data with various BSA concentrations. The phase retardation δ and normalized effective birefringence N was plotted against the concentration of BSA to demonstrate the positive correlation of these electro-optical parameters with the concentration of biomolecules.

$$\delta = \frac{2\pi d \Delta n_{\text{eff}}}{\lambda}, \tag{1}$$

where λ, d, and Δn_{eff} represent the wavelength of the incident probe beam, cell gap, and the effective optical anisotropy of LC, respectively. To eliminate the variation in cell gap, the effective optical anisotropy Δn_{eff} thus obtained was normalized to that of the birefringence of the LC, Δn_{LC}, in the absence of BSA. The ratio is designated N as follows:

$$N = \frac{\Delta n_{\text{eff}}}{\Delta n_{\text{LC}}}. \tag{2}$$

When both δ and N were plotted against the concentration of BSA as shown in Fig. 4, a positive correlation was observed as expected, suggesting that these electro-optical parameters are positively related to the concentration of biomolecules present.

3.3 Voltage dependence of the electrical capacitance of LCs in the presence of various concentrations of BSA

The correlation between the electro-optical properties of LCs and the concentration of BSA was further explored by examining the electrical capacitance of the LC cell as a function of the externally applied ac voltage. In the presence of BSA, the electrical capacitance of the LC cell increased with increasing voltage and reached a plateau at high voltages (Fig. 5). It was observed that the higher the concentration of BSA, the greater the difference between the maximum and minimum capacitance in the voltage-dependent capacitance (C–V) curve. Note that the maximum capacitance was obtained at 15 V and the minimum at null voltage. Figure 6 depicts the BSA concentration dependence of the capacitance difference ΔC.

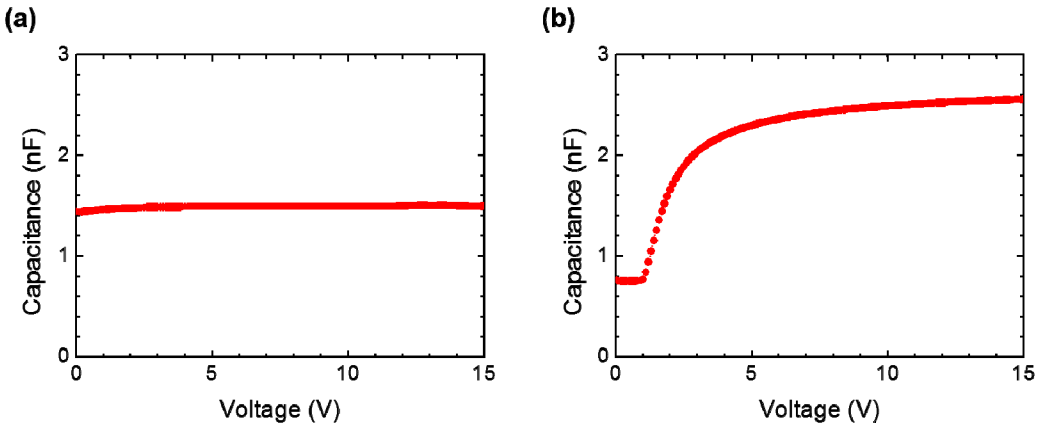

Figure 5. Voltage dependence of the electrical capacitance of LCs in the presence of (a) 0 and (b) 1 mg/ml of BSA spin-coated on DMOAP-coated ITO glass substrates. d = 10.2 ± 0.2 μm. The higher capacitance at 15 V in case (b) is primarily due to its smaller cell gap and even smaller thickness of the LC bulk.

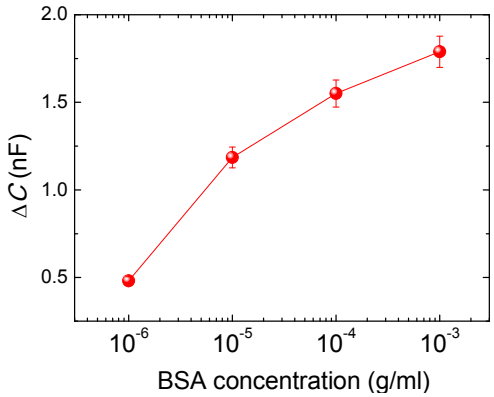

Figure 6. Correlation between the electric parameter ΔC of LCs derived from C–V measurement and the BSA concentration. ΔC is plotted against the concentration of BSA to show the positive correlation of the capacitance difference with the concentration of biomolecules.

4. CONCLUDING REMARKS

Current protein assay methods generally rely on colorimetric measurement to determine protein concentration. A calibration curve of spectroscopic absorbance versus BSA concentration is produced by linear regression to quantitate the concentration of protein samples. However, such linear correlation occurs within a limited range of BSA concentrations, for instance, 0.2–1.5 mg/ml, and may become imprecise at quantitating low concentrations of proteins. In this study, we explore the possibility of exploiting the electro-optical and electric capacitance properties of LCs in protein quantitation. Because the extent to which the alignment of LCs is disturbed is positively correlated with the amount of BSA present, it is reasoned that when an electric field is applied to restore the disrupted LC molecules to the vertical alignment, changes in the electro-optical and capacitance parameters of LCs may be useful in determining protein concentration. Results from the voltage–transmittance and voltage–capacitance measurements suggest that the parameters such as the phase retardation δ, reduced birefringence N, and the capacitance difference ΔC are positively correlated with BSA concentration. It is thus demonstrated that the approach developed in this study may serve as a potential quantitative method for a wider range of protein concentrations with higher accuracy for LC-based biosensing.

ACKNOWLEDGMENTS

The authors thank Mr. Yu-Chien Sung for his assistance with Fig. 1. This study is financial supported by the Ministry of Science and Technology, Taiwan, under grant Nos. 104-2112-M-009-008-MY3 and 101-2314-B-309-001-MY3.

REFERENCES

[1] Clare, B. H. and Abbott, N. L., "Orientations of nematic liquid crystals on surfaces presenting controlled densities of peptides: amplification of protein−peptide binding events," Langmuir 21(14), 6451–6461 (2005).
[2] Hartono, D., Xue, C.-Y., Yang, K.-L., and Yung, L.-Y. L., "Decorating liquid crystal surfaces with proteins for real-time detection of specific protein–protein binding," Adv. Funct. Mater. 19(22), 3574–3579 (2009).
[3] Kim, S. R. and Abbott, N. L., "Rubbed films of functionalized bovine serum albumin as substrates for the imaging of protein–receptor interactions using liquid crystals," Adv. Mater. 13(19), 1445–1449 (2001).
[4] Luk, Y. Y., Tingey, M. L., Hall, D. J., Israel, B. A., Murphy, C. J., Bertics, P. J., and Abbott, N. L., "Using liquid crystals to amplify protein-receptor interactions: design of surfaces with nanometer-scale topography that present histidine-tagged protein receptors," Langmuir 19(5), 1671–1680 (2003).
[5] Bi, X., Lai, S.-L., and Yang, K.-L., "Liquid crystal multiplexed protease assays reporting enzymatic activities as optical bar charts," Anal. Chem. 81(13), 5503–5509 (2009).
[6] Hoogboom, J., Velonia, K., Rasing, T., Rowan, A. E., and Nolte, R. J., "LCD-based detection of enzymatic action," Chem. Commun. (Camb) 434–435 (2006).
[7] Luk, Y. Y., Tingey, M. L., Dickson, K. A., Raines, R. T., and Abbott, N. L., "Imaging the binding ability of proteins immobilized on surfaces with different orientations by using liquid crystals," J. Am. Chem. Soc. 126(29), 9024–9032 (2004).
[8] Tingey, M. L., Wilyana, S., Snodgrass, E. J., and Abbott, N. L., "Imaging of affinity microcontact printed proteins by using liquid crystals," Langmuir 20(16), 6818–6826 (2004).
[9] Chen, C.-H., and Yang, K.-L., "Liquid crystal-based immunoassays for detecting hepatitis B antibody," Anal. Biochem. 421(1), 321–323 (2012).
[10] Kim, S. R., Shah, R. R., and Abbott, N. L., "Orientations of liquid crystals on mechanically rubbed films of bovine serum albumin: a possible substrate for biomolecular assays based on liquid crystals," Anal. Chem. 72(19), 4646–4653 (2000).
[11] Luk, Y. Y., Jang, C. H., Cheng, L. L., Israel, B. A., and Abbott, N. L., "Influence of lyotropic liquid crystals on the ability of antibodies to bind to surface-immobilized antigens," Chem. Mater. 17(19), 4774–4782 (2005).
[12] Xue, C.-Y., Khan, S. A. and Yang, K.-L., "Exploring optical properties of liquid crystals for developing label-free and high-throughput microfluidic immunoassays," Adv. Mater. 21(2), 198–202 (2009).
[13] Xue, C.-Y. and Yang, K.-L., "Dark-to-bright optical responses of liquid crystals supported on solid surfaces decorated with proteins," Langmuir 24(2), 563–567 (2008).

[14] Sun, S.-H., Lee, M.-J., Lee, Y.-H., Lee, W., Song, X., and Chen, C.-Y., "Mesogen of large birefringence enhances the sensitivity of liquid-crystal-based immunoassays for the cancer biomarker CA125," Biomed. Opt. Express 6(1), 245–256 (2015).
[15] Su, H.-W., Lee, Y.-H., Lee, M.-J., Hsu, Y.-C., and Lee, W., "Label-free immunodetection of the cancer biomarker CA125 using high-Δn liquid crystals," J. Biomed. Opt. 19(7), 077006 (2014).
[16] Su, H.-W., Lee, M.-J., and Lee, W., "Surface modification of alignment layer by ultraviolet irradiation to dramatically improve the detection limit of liquid-crystal-based immunoassay for the cancer biomarker CA125," J. Biomed. Opt. 20(5), 57004 (2015).
[17] Khan, M., and Park, S. Y., "Liquid crystal-based proton sensitive glucose biosensor," Anal. Chem. 86(3), 1493–1501 (2014).
[18] Yang, S., Liu, Y., Tan, H., Wu, C., Wu, Z., Shen, G. and Yu, R., "Gold nanoparticle based signal enhancement liquid crystal biosensors for DNA hybridization assays," Chem. Commun. (Camb.) 48(23), 2861–2863 (2012).
[19] Tan, H., Yang, S., Shen, G., Yu, R. and Wu, Z., "Signal-enhanced liquid-crystal DNA biosensors based on enzymatic metal deposition," Angew. Chem. Int. Ed. 49(46), 8608–8611 (2010).
[20] Tan, H., Li, X., Liao, S., Yu, R., and Wu, Z., "Highly-sensitive liquid crystal biosensor based on DNA dendrimers-mediated optical reorientation," Biosens. Bioelectron. 62, 84–89 (2014).